Arabian Journal for Science and Engineering
https://doi.org/10.1007/s13369-024-09697-w

RESEARCH ARTICLE-PHYSICS

Teleportation of Qubits in a Kicked Nonlinear Cavity with Ultra-short Pulses via Quantum Noisy Channels

Elsayed Barakat[1] · Amr Abd Al-Rahman Youssef[2] · I. L. El-Kalla[1] · M. Abdel-Aty[3,4,5]

Received: 21 December 2023 / Accepted: 9 October 2024

Abstract
In this paper, we delve into the profound ramifications of noise on qubit teleportation between the esteemed figures of Alice and Bob, ruthlessly quantifying the negativity and distance of the transmitted information. Through the invocation of an audacious modification to the Hamiltonian of the Jaynes–Cummings model, incorporating the ferocious power of a kicked cavity and ultra-short laser pulses, we unleash a tempest that unrelentingly shapes the entanglement and quality of the teleported information. Moreover, we fearlessly venture into the treacherous territory of noisy channels, including the formidable adversaries of phase flip and double phase flip channels, as they mercilessly assail the teleported state, engendered by the tumultuous interaction within the unforgiving depths of the kicked cavity, only to be met with our resolute projection.

Keywords Teleportation · Kicked cavity · Negativity · Distance

1 Introduction

The analysis of quantum algorithms based on entanglement measures is an important area of research in quantum computing [1]. Entanglement, a fundamental property of quantum systems, plays a crucial role in the efficiency, scalability, and robustness of quantum algorithms [2]. By studying entanglement measures, we gain insights into the computational power, resource requirements, and complexity of these algorithms. This analysis helps in understanding the role of entanglement in quantum tasks, identifying entanglement patterns, and developing new algorithms. Ultimately, it contributes to the advancement and optimization of quantum computing for various applications [3–6].

Quantum teleportation, a remarkable phenomenon in the field of quantum mechanics, holds great promise for secure communication and quantum computing, and recently, it is considered as an efficient tool in quantum neural network as it get rid of prior measurements on the output state [7]. However, one of the major challenges in implementing quantum teleportation lies in the presence of noisy channels [8–12]. Unfortunately, these channels can be noisy due to the interaction with the environment which causes a distortion in the delivered information [6, 13]. The study of noisy quantum channels has granted important results about quantum error-correction when the process depends on the entanglement between the sender and receiver qubits [14–18].

This followed by a successful demonstrated teleportation of qubits for optical coherent states and a photonic qubit [19, 20]. It is essential to prepare a pure maximally entangled state like the Bell state and a noiseless channel to have an ideal teleportation; however, this is almost a theoretical process due to the decoherence that coexists with the mixed quantum states. As a result, transmitting and receiving information under noisy channels may not be trusted since partial

✉ Elsayed Barakat
elsayedbarakat@mans.edu.eg

Amr Abd Al-Rahman Youssef
amraay2009@gmail.com

I. L. El-Kalla
al_kalla@mans.edu.eg

M. Abdel-Aty
mabdelaty@zewailcity.edu.eg

1 Mathematics and Engineering Physics Department, Faculty of Engineering, Mansoura University, Mansoura, Egypt

2 Mathematics from Faculty of Science Al-Azhar University, Cairo, Egypt

3 Deanship of Graduate Studies and Research, Ahlia University, P.O. Box 10878 Manama, Bahrain

4 Jadara Research Center, Jadara University, PO Box 733 Irbid, Jordan

5 Department of Mathematics, Faculty of Sciences, Jadara University, Irbid, Jordan

Published online: 30 October 2024

or degrade information may be lost during the communication process [21, 22]. One of the most common types of noisy channels is the phase flip channel in which the relative phase between the energy eigenstates of the system is lost. Also, the off-diagonal elements of the density matrix are decaying. This is considered to be a loss of information with no loss in energy.

The Jaynes–Cummings model and the Heisenberg model are two important theoretical frameworks in the field of quantum physics, each with its own significance in the context of quantum teleportation [23–27]. The Heisenberg model is a general framework used to describe the dynamics of interacting spin systems. In the context of quantum teleportation, the Heisenberg model can be used to analyze the behavior of entangled spin systems or spin chains. These spin systems can represent qubits, and their entanglement properties play a crucial role in the teleportation protocol. By studying the Heisenberg model, researchers can gain insights into the dynamics of entanglement transfer and manipulation within the spin systems involved in the teleportation process [28]. Indeed, the Jaynes–Cummings model is the best quantum model to describe the quantum features of the interaction between a single two-level atom with a single cavity mode in the presence of Kerr medium [29]. This model has been investigated in many literature studies, and nonclassical behaviors have been obtained [30–36]. Also, a lot of experiments have been done which lead to create entangled states that is a must in quantum computations and quantum teleportation [37–39]. In fact, the obstacle which faces any entangled states is the surviving time; however, some modifications in the nature of the electromagnetic filed can lead to a long lifetime survival [30, 40–43]. This model is particularly relevant in the study of quantum teleportation because it provides insights into the dynamics of entanglement generation and manipulation between qubits and photons. Previous works proved that different entanglement measurements like concurrence and negativity provide different values for the same quantum state [44, 45].

In this paper, we adopt the measures of distance and negativity to comprehensively analyze the quality and entanglement of the teleported state, respectively, as it journeys to its ultimate destination. We present a pioneering scheme that involves the periodic kicking of a cavity by a sequence of powerful classical laser pulses, in the presence of the Kerr nonlinearity, leading to a remarkable phase shift in the field. By employing a cavity containing a nonlinear Kerr medium, initially prepared in a coherent state, and subjecting it to a series of short laser pulses that linearly couple with the cavity field, we demonstrate the generation of a quantum state that can undergo further projection to significantly enhance its properties [46, 47].

In Sect. 2, a quantum model is chosen as a two-level atom and a boson in the coherent state under the classical magnetic field, Kerr medium and laser pulses. The wavefunction of a quantum model will be evaluated. Three forms of input state ρ_{in} are constructed under effect of a single laser pulse, two laser pulses, and three laser pulses, respectively. In Sect. 3, the quantum phase flip channel and the double quantum phase flip channel are selected in order to be achieved the teleportation. In Sect. 3, the quantum noise and entanglement are studied by the distance and the negativity in two channels. In Sect. 5, a brief summary is given.

2 The Model

In this section we will investigate the modified version of the Jaynes–Cummings model of a two-level system atom interacting with a cavity field, while this cavity is kicked with ultra-short laser pulses during the interaction. Under the rotating wave approximation, the model takes the form [46, 47]

$$H = \omega a^{\dagger}a + B\sigma_z + \chi a^{\dagger 2}a^2 + (a\sigma_+ + a^{\dagger}\sigma_-) \left[\xi_1 + \xi_2 \sum_{k=1}^{r} \delta(t - kT)\right], \quad (1)$$

where $a^{\dagger}(a)$ and $\sigma_+(\sigma_-)$ represent creation (annihilation) operator and raising (lowering) Pauli operators, respectively. (χ, ξ_1, ξ_2 and T) denotes nonlinearity of the Kerr medium, strength of the field-medium coupling and period of pulses, respectively. We assume that the atom is initially either in the excited state $|e\rangle$ or in the ground state $|g\rangle$; this can be described by the state $|\varpi, \phi\rangle = \cos\varpi\,|e\rangle + \mathbf{e}^{\mathbf{i}\phi}\sin\varpi\,|g\rangle$, where ϕ denotes the relative phase of the two atomic levels. Indeed, the wave function describes the atom in the excited state $|e\rangle$; we have to take ($\varpi = 0$) while for the atom being in the ground state $|g\rangle$ ($\varpi = \pi/2$). In the following, we will consider the field to be initially in coherent state given by $|\theta\rangle = \sum_{n=0}^{\infty} b_n|n\rangle$, where $b_n = \nu^{n/2}e^{-\nu/2}/\sqrt{n!}$ with ν denotes the intensity of the initial coherent field. Now assume the wavefunction takes the form [48]

$$|\Psi\rangle_{AF} = \sum_{n=0}^{\infty} \left(\Psi_{e,n}(t)\,|e,n\rangle + \Psi_{g,n+1}(t)\,|g,n+1\rangle\right), \quad (2)$$

where $\Psi_{e,n}$ and $\Psi_{g,n+1}$ are complex amplitudes of states $|e,n\rangle$ and $|g,n+1\rangle$, respectively, with initial conditions $\Psi_{e,n}(0) = b_n\cos\varpi$, $\Psi_{g,n+1}(0) = b_{n+1}\mathbf{e}^{\mathbf{i}\phi}\sin\varpi$; $n = 0, 1, 2, 3, \ldots$, and $\Psi_{g,0}(0) = 0$, where with rotating wave approximation we then substitute in Schrödinger equation $\frac{\partial}{\partial t}|\Psi(t)\rangle = -\mathbf{i}H|\Psi(t)\rangle$ to get:

$$\frac{\partial \Psi_{e,n}}{\partial t} = -\mathbf{i}\Delta_1\Psi_{e,n}(t) - \mathbf{i}\xi_1\sqrt{n+1}\Psi_{g,n+1}(t)$$

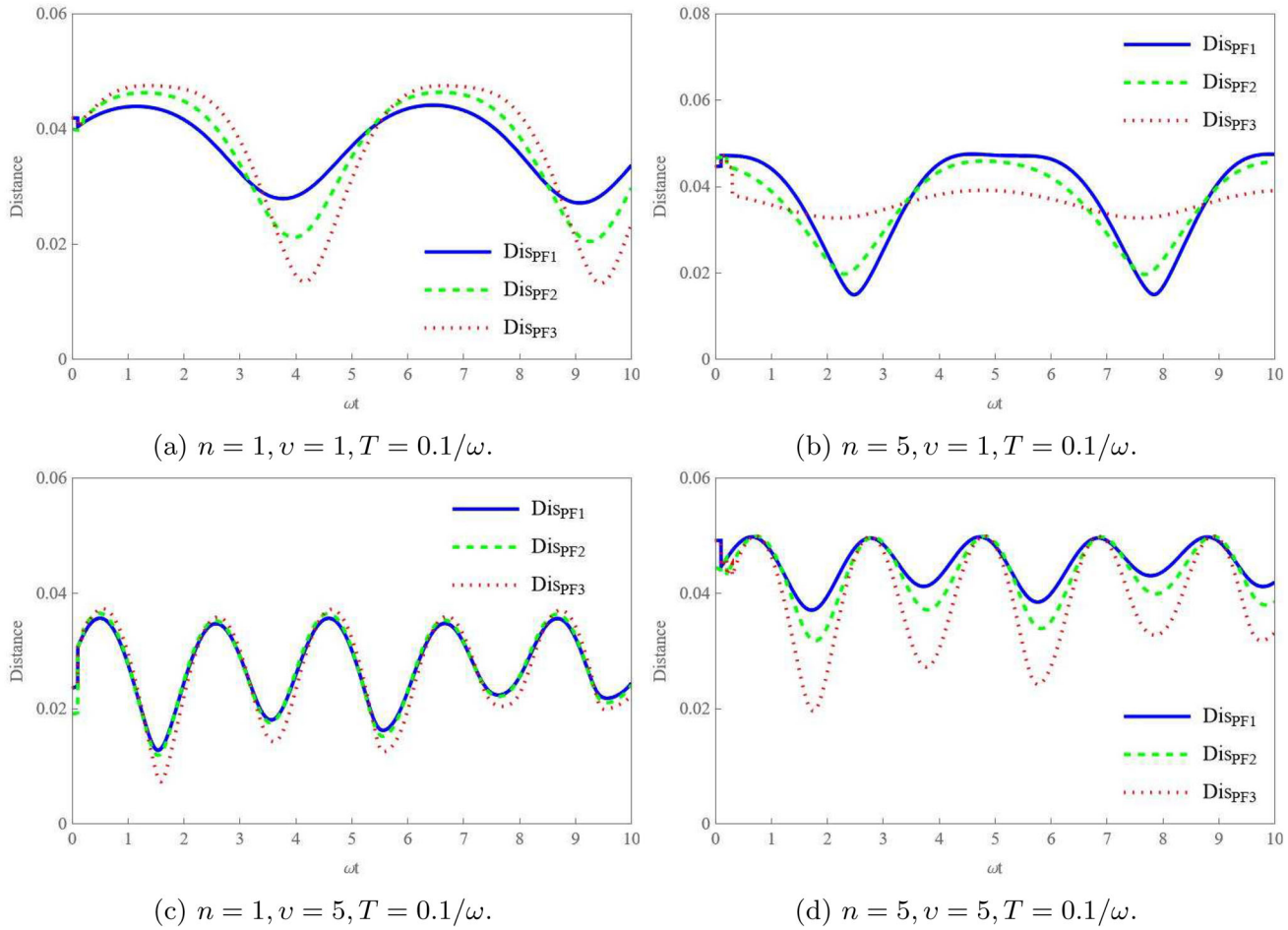

(a) $n = 1, \upsilon = 1, T = 0.1/\omega$. (b) $n = 5, \upsilon = 1, T = 0.1/\omega$.

(c) $n = 1, \upsilon = 5, T = 0.1/\omega$. (d) $n = 5, \upsilon = 5, T = 0.1/\omega$.

Fig. 1 Time evolution of distance for quantum phase flip channel

$$-\mathbf{i}\xi_2 \sum_{k=1}^{r} \sqrt{n+1}\delta(t-kT)\Psi_{g,n+1}(t) \tag{3}$$

$$\frac{\partial \Psi_{g,n+1}}{\partial t} = -\mathbf{i}\Delta_2 \Psi_{g,n+1}(t) - \mathbf{i}\xi_1\sqrt{n+1}\Psi_{e,n}(t) - \mathbf{i}\xi_2 \sum_{k=1}^{r} \sqrt{n+1}\delta(t-kT)\Psi_{e,n}(t) \tag{4}$$

where $\Delta_1 = \omega(n+1) + \chi n(n-1) + B$, and $\Delta_2 = \omega(n+1) + \chi n(n+1) - B$ are real constants. Complex amplitudes $\Psi_{e,n}(t)$ and $\Psi_{g,n+1}(t)$ are solutions of Eqs. 3, 4 and are formulated as:

$$\begin{aligned}\Psi_{e,n}(t) &= \mathbf{e}^{-\mathbf{i}(\Delta_1+\Delta_2)t/2}\left(\Psi_{e,n}(0)\cos(\frac{\mu_0 t}{2}) - \mathbf{i}\mu_1\sin(\frac{\mu_0 t}{2})\right) \\ &-\mathbf{i}\frac{\xi_1\xi_2(n+1)}{\mu_0}\sum_{k=1}^{r}\Psi_{e,n}(kT)\,\mathbf{e}^{-\mathbf{i}(\Delta_1+\Delta_2+\mu_0)(t-kT)/2} \\ &(1-\mathbf{e}^{-\mathbf{i}\mu_0(t-kT)})u(t-kT) \\ &-\xi_2\sqrt{n+1}\sum_{k=1}^{r}\Psi_{g,n+1}(kT)\,\mathbf{e}^{-\mathbf{i}(\Delta_1+\Delta_2)(t-kT)/2} \\ &\times\left(\frac{(\Delta_1-\Delta_2)}{\mu_0}\sin\left(\frac{\mu_0}{2}(t-kT)\right)\right. \\ &\left.+\mathbf{i}\cos\left(\frac{\mu_0}{2}(t-kT)\right)\right)u(t-kT),\end{aligned} \tag{5}$$

and

$$\begin{aligned}\Psi_{g,n+1}(t) &= \mathbf{e}^{-\mathbf{i}(\Delta_1+\Delta_2)t/2}\left(\Psi_{g,n+1}(0)\cos(\frac{\mu_0 t}{2})\right. \\ &\left.+\mathbf{i}\mu_2\sin(\frac{\mu_0 t}{2})\right) \\ &-\mathbf{i}\frac{\xi_1\xi_2(n+1)}{\mu_0}\sum_{k=1}^{r}\Psi_{g,n+1}(kT)\,\mathbf{e}^{-\mathbf{i}(\Delta_1+\Delta_2+\mu_0)(t-kT)/2} \\ &(1-\mathbf{e}^{-\mathbf{i}\mu_0(t-kT)})u(t-kT) \\ &-\xi_2\sqrt{n+1}\sum_{k=1}^{r}\Psi_{e,n}(kT)\,\mathbf{e}^{-\mathbf{i}(\Delta_1+\Delta_2)(t-kT)/2} \\ &\times\left(\frac{(\Delta_1-\Delta_2)}{\mu_0}\sin\left(\frac{\mu_0}{2}(t-kT)\right)\right. \\ &\left.-\mathbf{i}\cos\left(\frac{\mu_0}{2}(t-kT)\right)\right)u(t-kT),\end{aligned} \tag{6}$$

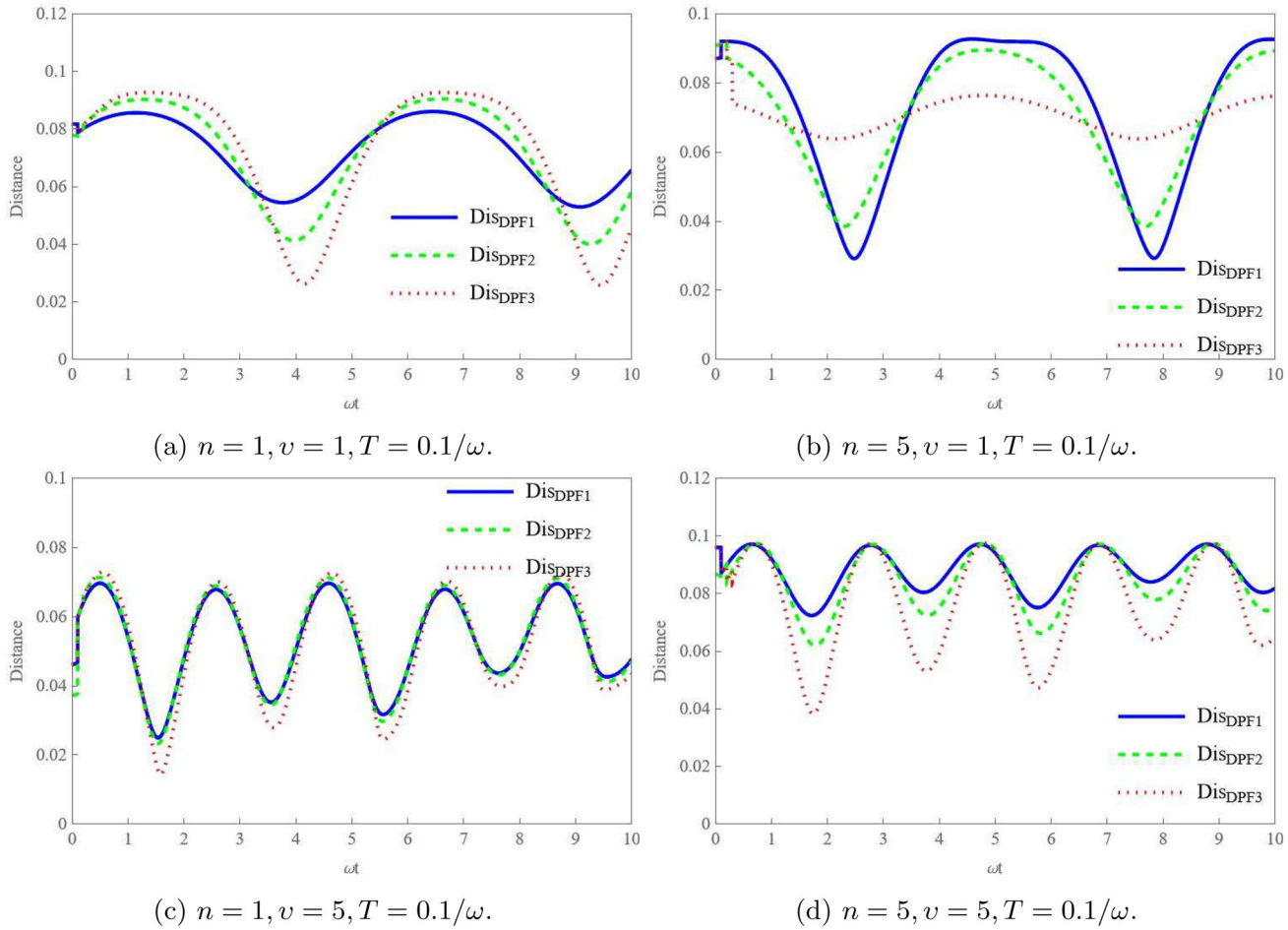

(a) $n = 1, \upsilon = 1, T = 0.1/\omega$. (b) $n = 5, \upsilon = 1, T = 0.1/\omega$.

(c) $n = 1, \upsilon = 5, T = 0.1/\omega$. (d) $n = 5, \upsilon = 5, T = 0.1/\omega$.

Fig. 2 Time evolution of distance for quantum double phase flip channel

where real constant $\mu_0 = \sqrt{(\Delta_1 - \Delta_2)^2 + 4(n+1)\xi_1^2}$, $\mu_1 = \left((\Delta_1 - \Delta_2)\Psi_{e,n}(0) + 2\sqrt{n+1}\xi_1\Psi_{g,n+1}(0)\right)/\mu_0$, and $\mu_2 = ((\Delta_1 - \Delta_2)\Psi_{g,n+1}(0) - 2\sqrt{n+1}\xi_1\Psi_{e,n}(0))/\mu_0$, and the unit step function $u(t - kT)$ is defined as [49]:

$$u(t-kT) = \begin{cases} 1, t \geq kT \\ 0, t < kT \end{cases}, k = 0, 1, 2, 3, \ldots \tag{7}$$

It is important that complex amplitude values of excited and ground states $\Psi_{e,n}(kT)$ and $\Psi_{g,n+1}(kT)$ are later computed by initial conditions $\Psi_{e,n}(0)$ and $\Psi_{g,n+1}(0)$ at the time $t = KT; k = 1, 2, 3, \ldots, r$. Values of $\Psi_{e,n}(kT)$ and $\Psi_{g,n+1}(kT)$ are found successively in terms of values of $\Psi_{e,n}((k-1)T), \Psi_{e,n}((k-2)T), \ldots, \Psi_{e,n}(T), \Psi_{e,n}(0)$, $\Psi_{g,n+1}((k-1)T)$, $\Psi_{g,n+1}((k-2)T)$, $\ldots$, $\Psi_{g,n+1}(T)$, $\Psi_{g,n+1}(0)$ for k laser pulses. Hence, for the first laser pulse, amplitudes $\Psi_{e,n}(T)$, and $\Psi_{g,n+1}(T)$ are expressed as:

$$\begin{aligned}
\Psi_{e,n}(T) = &-\frac{(\Psi_{e,n}(0) - \mathbf{i}\xi_2\sqrt{n+1}\Psi_{g,n+1}(0))}{(n+1)\xi_2^2 - 1}\mathbf{e}^{-\mathbf{i}(\Delta_1+\Delta_2)T/2} \\
&\cos(\frac{\mu_0 T}{2}) \\
&-\frac{(\xi_2\sqrt{n+1}\mu_2 - \mathbf{i}\mu_1)}{(n+1)\xi_2^2 - 1}\mathbf{e}^{-\mathbf{i}(\Delta_1+\Delta_2)T/2}\sin(\frac{\mu_0 T}{2}), \\
\Psi_{g,n+1}(T) = &-\frac{(\Psi_{g,n+1}(0) + \mathbf{i}\xi_2\sqrt{n+1}\Psi_{e,n}(0))}{(n+1)\xi_2^2 - 1}\mathbf{e}^{-\mathbf{i}(\Delta_1+\Delta_2)T/2} \\
&\cos(\frac{\mu_0 T}{2}) \\
&-\frac{(\xi_2\sqrt{n+1}\mu_1 + \mathbf{i}\mu_2)}{(n+1)\xi_2^2 - 1}\mathbf{e}^{-\mathbf{i}(\Delta_1+\Delta_2)T/2}\sin(\frac{\mu_0 T}{2}),
\end{aligned} \tag{8}$$

For two laser pulses, amplitudes values $\Psi_{e,n}(2T)$ and $\Psi_{g,n+1}(2T)$ are taken as:

$$\begin{aligned}
\Psi_{e,n}(2T) &= -\frac{\left(c_1 + \mathbf{i}\xi_2\sqrt{n+1}c_2\right)}{(n+1)\xi_2^2 - 1}, \\
\Psi_{g,n+1}(2T) &= -\frac{\left(c_2 + \mathbf{i}\xi_2\sqrt{n+1}c_1\right)}{(n+1)\xi_2^2 - 1},
\end{aligned} \tag{9}$$

where

$$\begin{aligned}
c_1 = &\mathbf{e}^{-\mathbf{i}(\Delta_1+\Delta_2)T}\left(\Psi_{e,n}(0)\cos(\mu_0 T) - \mathbf{i}\mu_1\sin(\mu_0 T)\right) \\
&-\mathbf{i}\frac{\xi_1\xi_2(n+1)}{\mu_0}\Psi_{e,n}(T)\,\mathbf{e}^{-\mathbf{i}(\Delta_1+\Delta_2+\mu_0)T/2}(1 - \mathbf{e}^{-\mathbf{i}\mu_0 T})u(T)
\end{aligned}$$

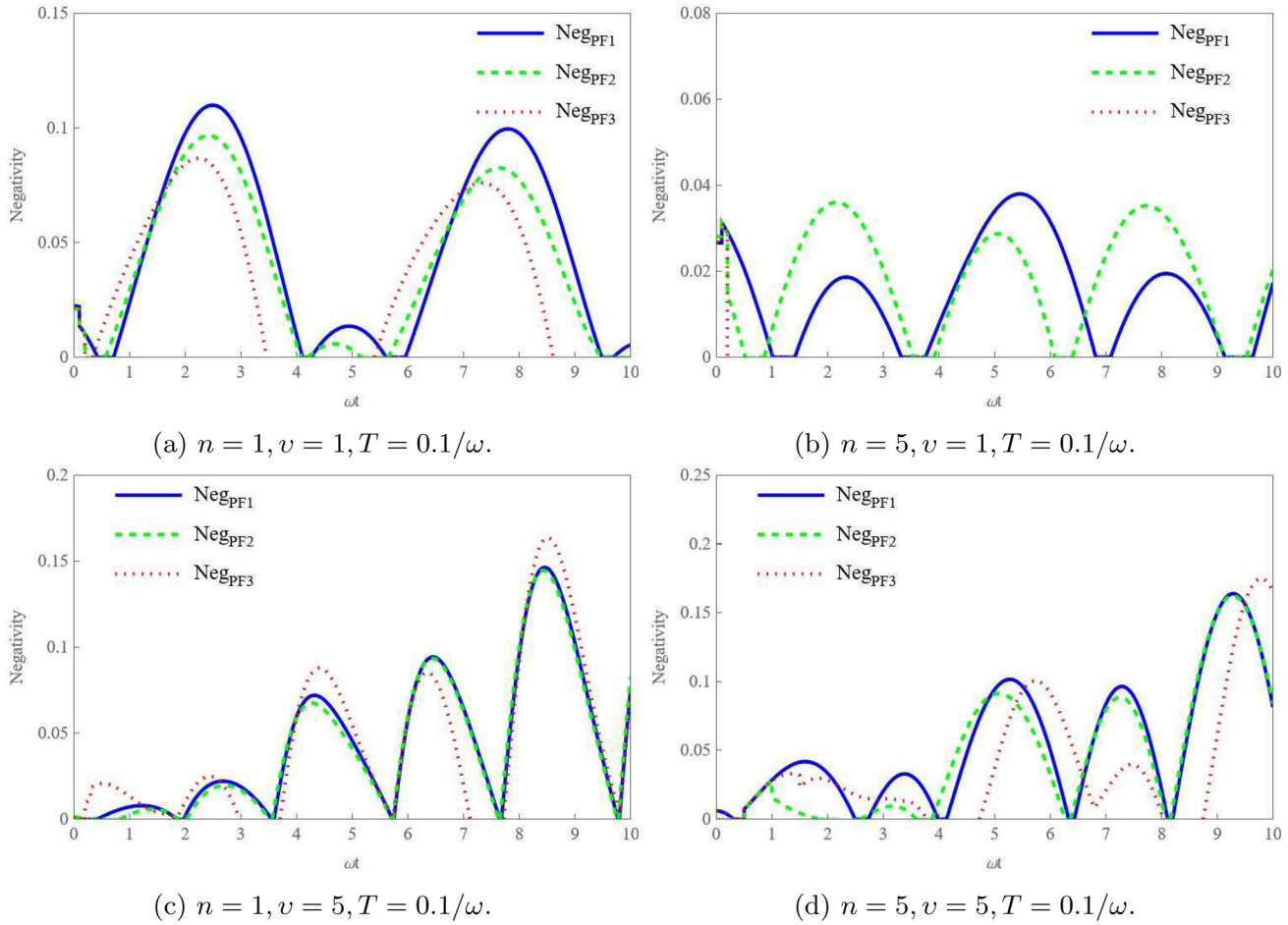

(a) $n = 1, \upsilon = 1, T = 0.1/\omega$. (b) $n = 5, \upsilon = 1, T = 0.1/\omega$.

(c) $n = 1, \upsilon = 5, T = 0.1/\omega$. (d) $n = 5, \upsilon = 5, T = 0.1/\omega$.

Fig. 3 Time evolution of negativity for quantum phase flip channel

$$-\xi_2\sqrt{n+1}\Psi_{g,n+1}(T)\,\mathbf{e}^{-\mathbf{i}(\Delta_1+\Delta_2)T/2}\left(\frac{(\Delta_1-\Delta_2)}{\mu_0}\sin(\frac{\mu_0 T}{2})\right.$$
$$\left.+\mathbf{i}\cos(\frac{\mu_0 T}{2})\right)u(T), \tag{10}$$

and

$$c_2 = \mathbf{e}^{-\mathbf{i}(\Delta_1+\Delta_2)T}\left(\Psi_{g,n+1}(0)\cos(\mu_0 T)+\mathbf{i}\mu_2\sin(\mu_0 T)\right)$$
$$-\mathbf{i}\frac{\xi_1\xi_2(n+1)}{\mu_0}\Psi_{g,n+1}(T)\,\mathbf{e}^{-\mathbf{i}(\Delta_1+\Delta_2+\mu_0)T/2}(1-\mathbf{e}^{-\mathbf{i}\mu_0 T})u(T)$$
$$-\xi_2\sqrt{n+1}\Psi_{e,n}(T)\,\mathbf{e}^{-\mathbf{i}(\Delta_1+\Delta_2)T/2}\left(\frac{(\Delta_1-\Delta_2)}{\mu_0}\sin(\frac{\mu_0 T}{2})\right.$$
$$\left.-\mathbf{i}\cos(\frac{\mu_0 T}{2})\right)u(T), \tag{11}$$

For three laser pulses, amplitudes values $\Psi_{e,n}(3T)$ and $\Psi_{g,n+1}(3T)$ are determined by:

$$\Psi_{e,n}(3T) = -\frac{\left(c_3+\mathbf{i}\xi_2\sqrt{n+1}c_4\right)}{(n+1)\,\xi_2^2-1},$$
$$\Psi_{g,n+1}(3T) = -\frac{\left(c_4+\mathbf{i}\xi_2\sqrt{n+1}c_3\right)}{(n+1)\,\xi_2^2-1}, \tag{12}$$

$$c_3 = \mathbf{e}^{-3\mathbf{i}(\Delta_1+\Delta_2)T/2}\left(\Psi_{e,n}(0)\cos(\frac{3\mu_0 T}{2})\right.$$
$$\left.-\mathbf{i}\mu_1\sin(\frac{3\mu_0 T}{2})\right)$$
$$-\mathbf{i}\frac{\xi_1\xi_2(n+1)}{\mu_0}\sum_{k=1}^{2}\Psi_{e,n}(kT)\,\mathbf{e}^{-\mathbf{i}(\Delta_1+\Delta_2+\mu_0)(3T-kT)/2}$$
$$(1-\mathbf{e}^{-\mathbf{i}\mu_0(3T-kT)})u(3T-kT)$$
$$-\xi_2\sqrt{n+1}\sum_{k=1}^{2}\Psi_{g,n+1}(kT)\,\mathbf{e}^{-\mathbf{i}(\Delta_1+\Delta_2)(3T-kT)/2}$$
$$\times\left(\frac{(\Delta_1-\Delta_2)}{\mu_0}\sin\left(\frac{\mu_0}{2}(3T-kT)\right)\right.$$
$$\left.+\mathbf{i}\cos\left(\frac{\mu_0}{2}(3T-kT)\right)\right)u(3T-kT), \tag{13}$$

and

$$c_4 = \mathbf{e}^{-3\mathbf{i}(\Delta_1+\Delta_2)T/2}\left(\Psi_{g,n+1}(0)\cos(\frac{3\mu_0 T}{2})\right.$$

$$+\mathbf{i}\mu_2 \sin(\frac{3\mu_0 T}{2})\Big)$$
$$-\mathbf{i}\frac{\xi_1\xi_2\,(n+1)}{\mu_0}\sum_{k=1}^{2}\Psi_{g,n+1}\,(kT)\,\mathbf{e}^{-\mathbf{i}(\Delta_1+\Delta_2+\mu_0)(3T-kT)/2}$$
$$(1-\mathbf{e}^{-\mathbf{i}\mu_0(3T-kT)})u\,(3T-kT)$$
$$-\xi_2\sqrt{n+1}\sum_{k=1}^{2}\Psi_{e,n}\,(kT)\,\mathbf{e}^{-\mathbf{i}(\Delta_1+\Delta_2)(3T-kT)/2}$$
$$\times\left(\frac{(\Delta_1-\Delta_2)}{\mu_0}\sin\left(\frac{\mu_0}{2}(3T-kT)\right)\right.$$
$$\left.-\mathbf{i}\cos\left(\frac{\mu_0}{2}(3T-kT)\right)\right)u\,(3T-kT)\,, \tag{14}$$

We aim to prepare an input state which is sent through noisy quantum channels based on the state of joint atom–field $|\Psi(t)\rangle_{AF}$ (2). Geometrically, the density state of joint atom–field $\rho_{AF} = |\Psi(t)\rangle_{AF}\langle\Psi(t)|$ is represented by the $2\times\infty-$dimensional Hilbert space where $2-$dimensional Hilbert space describes geometrically the atom and the $\infty-$dimensional Hilbert space describes the field. The noisy quantum channels are formed by the $2\times 2-$dimensional Hilbert space. Therefore, the density state ρ_{AF} is inadequate for noisy quantum channels. Consequently, it is described geometrically by $2\times 2-$ dimensional Hilbert subspace. According to the density state ρ_{AF}, the input state is constructed physically as the two hybrid qubits; the first qubit is an atom, and the second qubit is the photon. Subsequently, the $2\times 2-$dimensional Hilbert subspace depends on the set of vector bases $\{|n,g\rangle, |n+1,g\rangle, |n,e\rangle, |n+1,e\rangle; n\geq 1\}$ based on the two photon states $|n\rangle$, and $|n+1\rangle$ of the field and the ground and excited states $|g\rangle$, and $|e\rangle$ of the atom, respectively. Consequently, we form projectors $P_{(n+1)g,(n+1)g}$, $P_{ne,ne}$, and $P_{(n+1)g,ne}$; $n\geq 0$, by local actions where the projector is $P_{ij} = p_{ij}\,|j\rangle\langle i|$ and $p_{ij} = \langle i|\rho_{af}|j\rangle$. Thus, values of projectors are given by $p_{(n+1)g,(n+1)g} = |\Psi_{g,n+1}|^2$, $p_{ne,ne} = |\Psi_{e,n}|^2$, $P_{(n+1)g,ne} = \Psi_{g,n+1}\Psi^*_{e,n}$, and $p_{ng,(n+1)e} = \Psi_{g,n}\Psi^*_{e,n+1}$ such that $n\geq 1$. Thus, projectors $P_{(n+1)g,(n+1)g}$, $P_{ne,ne}$, and $P_{(n+1)g,ne}$, and $P_{ng,(n+1)e}$; $n\geq 1$ are used to form the input state in the standard bases as:

$$\rho_{\text{in}} = f_1|00\rangle\langle 00| + f_2|01\rangle\langle 01| + f_3|10\rangle\langle 10| + f_4|11\rangle\langle 11|$$
$$+f_5|00\rangle\langle 11| + f_5^*|11\rangle\langle 00| + f_6|01\rangle\langle 10| + f_6^*|10\rangle\langle 01|, \tag{15}$$

where $f_1 = A^{-1}|\Psi_{g,n}|^2$, $f_2 = A^{-1}|\Psi_{e,n}|^2$, $f_3 = A^{-1}|\Psi_{g,n+1}|^2$, $f_4 = A^{-1}|\Psi_{e,n+1}|^2$, $f_5 = A^{-1}\Psi^*_{g,n}\Psi_{e,n+1}$, and $f_6 = A^{-1}\Psi_{g,n+1}\Psi^*_{e,n}$, such that $f_1+f_2+f_3+f_4 = 1$, the normalization constant A is taken as $A = |\Psi_{g,n}|^2 + |\Psi_{g,n+1}|^2 + |\Psi_{e,n}|^2 + |\Psi_{e,n+1}|^2$; $n\geq 1$, and bases $|n\rangle$, and $|g\rangle$ are renamed $|0\rangle$, while bases $|n+1\rangle$, and $|e\rangle$ changed, namely $|1\rangle$. We rewrite the set bases $\{|n,g\rangle, |n,e\rangle, |n+1,g\rangle, |n+1,e\rangle\}$ of $2\times 2-$dimensional Hilbert subspace in the set of standard bases $\{|0,0\rangle, |0,1\rangle, |1,0\rangle, |1,1\rangle\}$.

3 Quantum Phase Flip Channel

In this section, we intend to investigate the effect of local noisy environments on the evolution of two above input states which were discussed in the previous section. Input state ρ_{in} is sent through different noisy quantum channels with a decoherence parameter λ. Consequently, each quantum channel is investigated alone under parameters ϖ, ϕ, ν, ω, B, χ, ξ_1, ξ_2, r, T, and λ. Based on the approach of Kraus operators, noisy quantum channels of two qubits given by a density state ρ_{in} which affects one of two qubits can be given as [50, 51]:

$$\Lambda_{\text{out}} = \sum_i E_i\,\rho_{\text{in}}\,E_i{}^{\dagger}. \tag{16}$$

$$\Omega_{\text{out}} = \sum_{i,j}\left(E_i\otimes E_j\right)\rho_{\text{in}}\left(E_i\otimes E_j\right)^{\dagger}. \tag{17}$$

where Λ_{out} and Ω_{out} represent output states of the noisy quantum channels under suitable local decoherence Kraus operators E_i satisfying the completeness relation $\sum_i E_i^{\dagger}E_i = I$, where I is the 2×2 identity matrix.

Currently, the input state ρ_{in} (15) is teleported through the quantum phase flip channel and the quantum double phase flip channel which are expressed in terms of local Kraus operators $E_{\text{PF1}} = \sqrt{1-\lambda}I$, $E_{\text{PF2}} = \sqrt{\lambda}\,|0\rangle\langle 0|$, and $E_{\text{PF3}} = \sqrt{\lambda}\,|1\rangle\langle 1|$ as Eqs. 16, 17. The output states Λ_{PF}, and Ω_{DPF}, (18, 19) can be written in what follows:

$$\Lambda_{\text{PF}}(\rho_{\text{in}}) = f_1|00\rangle\langle 00| + f_2|01\rangle\langle 01|$$
$$+f_3|10\rangle\langle 10| + f_4|11\rangle\langle 11|$$
$$+(1-\lambda)\left(f_5|00\rangle\langle 11| + f_5^*|11\rangle\langle 00|\right.$$
$$\left.+f_6|01\rangle\langle 10| + f_6^*|10\rangle\langle 01|\right). \tag{18}$$

and

$$\Omega_{\text{DPF}}(\rho_{\text{in}}) = f_1|00\rangle\langle 00| + f_2|01\rangle\langle 01|$$
$$+f_3|10\rangle\langle 10| + f_4|11\rangle\langle 11|$$
$$+(1-\lambda)^2\left(f_5|00\rangle\langle 11| + f_5^*|11\rangle\langle 00|\right.$$
$$\left.+f_6|01\rangle\langle 10| + f_6^*|10\rangle\langle 01|\right). \tag{19}$$

In two output states Λ_{PF}, and Ω_{DPF}, f_1, f_2, f_3, and f_4 remain without change in their values but f_5 and f_5^* are contracted with $1-\lambda$ for Λ_{PF}, and $(1-\lambda)^2$ for Ω_{DPF}. Clearly, the quantum informational data f_5 and f_5^* weaken in Ω_{DPF} comparison with Λ_{PF}.

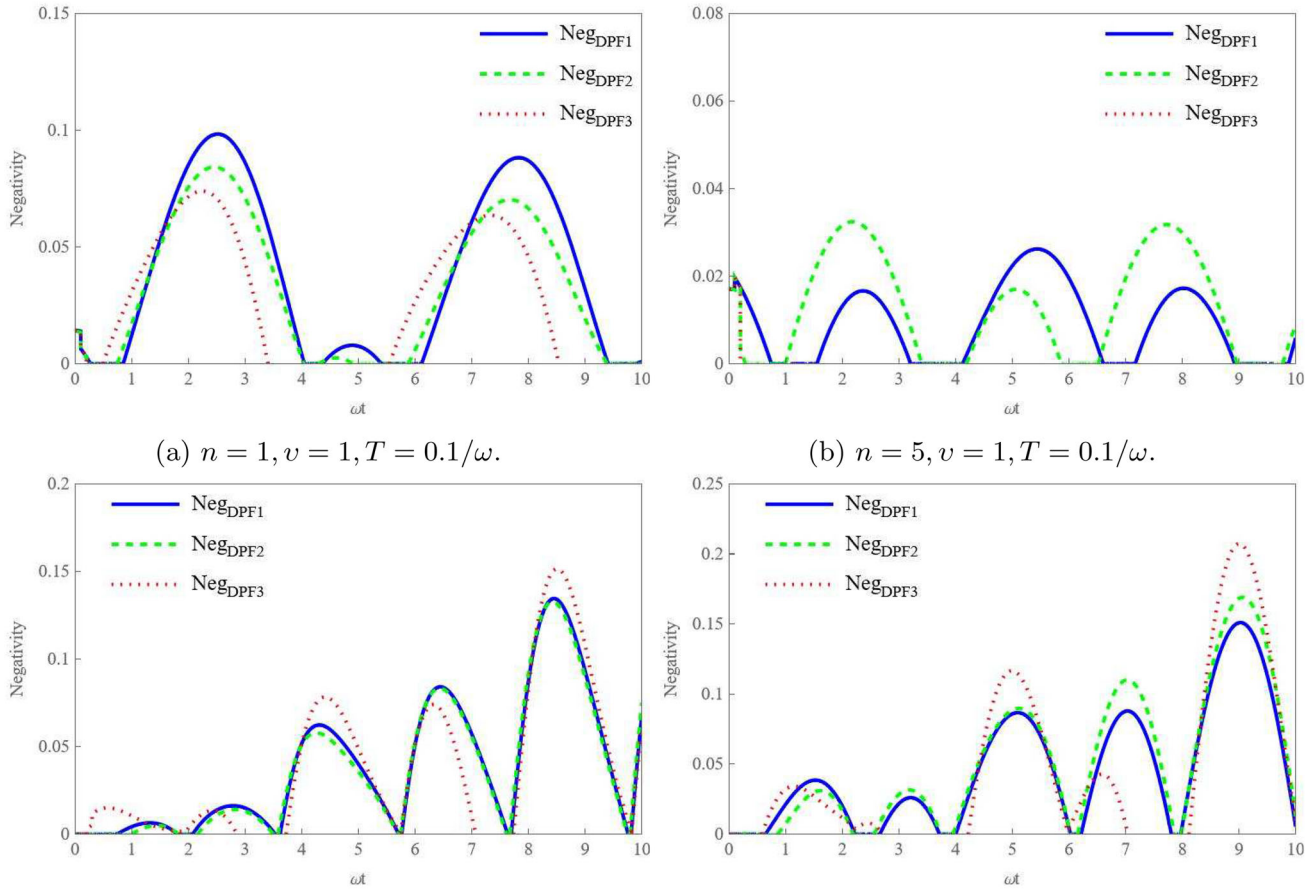

(a) $n = 1, \upsilon = 1, T = 0.1/\omega$. (b) $n = 5, \upsilon = 1, T = 0.1/\omega$.

(c) $n = 1, \upsilon = 5, T = 0.1/\omega$. (d) $n = 5, \upsilon = 5, T = 0.1/\omega$.

Fig. 4 Time evolution of negativity for quantum double phase flip channel

4 Discussion and Results

In the preceding sections, the quantum model consists of a two-level atom and a boson in the coherent state which is exposed to the classical magnetic field, Kerr medium and laser pulses. It is provided by the Hamiltonian (1) and is treated analytically in detail to find the time evolution of the wavefunction as above. The input state ρ_{in} (15) is prepared to be transferred through two noisy quantum channels. Here, two quantum noisy channels are the quantum phase flip channel and the double quantum phase flip channel. A proposed study of two noisy quantum channels recognizes characters of the quantum noises in environments of two channels with the input state ρ_{in}. In this section, characters of the quantum noise are analyzed by two quantum measurements: the distance and negativity. The distance D is a good measure for the quantum noise between input and output states ρ_{in} and ρ_{out} which is introduced as:

$$D\left(\rho_{\text{in}}, \rho_{\text{out}}\right) = \frac{1}{2}||\rho_{\text{out}} - \rho_{\text{in}}||_1. \tag{20}$$

where $||O||_1 = Tr\sqrt{O^{\dagger}O}$. The negativity is an accuracy measure for the entanglement and is given by:

$$N = \frac{||\rho_{\text{out}}^{T_1}||_1 - 1}{2}. \tag{21}$$

where $\rho_{\text{out}}^{T_1}$ is the partial transpose of the state ρ_{out}.

In all figures, parameters of the Hamiltonian and decoherence parameter of two channels are $\varpi = \pi/4$, $\phi = 0$, $\chi = 0.1$, $\xi_1 = 0.3$, $\xi_2 = 0.2$ and $\lambda = 0.05$. The distance measure is firstly discussed in Figs. 1 and 2, and the negativity is discussed later in Figs. 3 and 4 for two channels. The distance and negativity are plotted versus the scaled time ωt for two channels. Figures 1 and 3 are related to the quantum phase flip channel, and Figs. 2 and 4 are related to the double quantum phase flip channel. Each main figure has four figures according to parameter values of $n = 1$ and 5, $\nu = 1$ and 5, and $T = 0.1/\omega$. Hence, Fig. 1a–d is plotted at values ($n = 1$, $\nu = 1, T = 0.1/\omega$), ($n = 1$, $\nu = 5, T = 0.1/\omega$), ($n = 5$, $\nu = 1, T = 0.1/\omega$) and ($n = 5$, $\nu = 5, T = 0.1/\omega$), respectively. Influences of n, ν, and T parameters appear clearly

on behaviors of both of the distance and the negativity. In each figure, there are three curves: bold, dashed, and dotted curves which correspond to a single laser pulse, two laser pulses and three laser pulses, respectively. The scaled time ωt varies always from 0 to 10 in all figures, while ranges change from a figure to another. Currently, we discuss and analyze figures geometrically and physically for more details.

Figure 1 illustrates the examination of the quantum noise in the quantum phase flip channel through the distance between the input state ρ_{in} and the output state $\Lambda_{\text{PF}}(\rho_{\text{in}})$. The bold, dashed and dotted curves, denoted as Dis_{PF1}, Dis_{PF2} and Dis_{PF3}, respectively, depict the variations. As the coherence parameter of the electromagnetic field ν increases, the three curves exhibit rapid oscillations. Also, for a single photon $n = 1$ the three curves coincide that means the effect of the electromagnetic field overcomes the laser pulses effect. With increasing n, the three curves contract vertically; inasmuch, the effect of increasing the laser pulses is notable as it decreases the distance for three pulses case. The ranges of curves decrease with n and increase with ν.

In Fig. 2, the quantum double phase flip channel is investigated, and the quantum noise is analyzed based on the distance between the input state ρ_{in} and the output state $\Omega_{\text{DPF}}(\rho_{\text{in}})$. The bold, dashed and dotted curves, symbolically represented as Dis_{DPF1}, Dis_{DPF2} and Dis_{DPF3}, respectively, depict the variations. Figure 2 exhibits a similar pattern to Fig. 1, with the same parameter values of n, ν and T, but the ranges differ, with Fig (2) having the greatest ranges, so the phase flip channel is much efficient than double phase flip channel.

Figures 3 and 4 delve into a detailed analysis of entanglement, employing the negativity measure between the input state ρ_{in} and the output state $\Lambda_{\text{PF}}(\rho_{\text{in}})$ through the quantum phase flip channel and the quantum double phase flip channel, respectively. The entanglement is precisely and accurately measured using bold, dashed and dotted curves denoted as Neg_{PF1}, Neg_{PF2} and Neg_{PF3}, respectively. In Fig. 3a, the three curves progressively display varying levels of entanglement, with $\text{Neg}_{\text{PF3}} < \text{Neg}_{\text{PF2}} < \text{Neg}_{\text{PF1}}$. Notably, the curve representing a single laser pulse, Neg_{PF1}, exhibits the highest degree of entanglement, while the curve representing three laser pulses, Neg_{PF2}, demonstrates the lowest entanglement. Figure 3a also shows a sudden drop in entanglement for Neg_{PF3}. In Fig. 3b, curve Neg_{PF3} emerges as ωt approaches zero and disappears over the scaled time period at $n = 5$, while curves Neg_{PF1} and Neg_{PF2} exhibit maximal entanglement with the smallest range. Thus, as n increases, the entanglement decreases when comparing Fig. 3a. In Fig. 3c, when $\nu = 5$ and $T = 0.1/\omega$, all curves exhibit astounding oscillations, with Neg_{PF3} displaying the highest entanglement and the other two curves coinciding. In Fig. 3d, all curves demonstrate an ascending trend in entanglement, reaching maximum peaks. As n increases, the entanglement diminishes, while larger values of ν lead to increased entanglement, particularly for the Neg_{PF3} curve.

Similarly, in Fig. 4, the entanglement of the quantum double phase flip channel is investigated, with the negativity between the input state ρ_{in} and the output state $\Omega_{\text{DPF}}(\rho_{\text{in}})$ represented by bold, dashed and dotted curves denoted as Neg_{DPF1}, Neg_{DPF2} and Neg_{DPF3}, respectively. The behaviors of the Neg_{DPF1}, Neg_{DPF2} and Neg_{DPF3} curves in Fig. 4 mirror those of the Neg_{PF1}, Neg_{PF2} and Neg_{PF3} curves in Fig. 4, respectively.

Obviously, the distance is generally low in two channels. Consequently, output states $\Lambda_{\text{PF}}(\rho_{\text{in}})$ and $\Omega_{\text{DPF}}(\rho_{\text{in}})$ are nearly close to the input state ρ_{in}. Thus, the quantum noise is accessible in two channels. Also, the quantum noise of the quantum phase flip channel is less than in the quantum double phase flip channel. In other way, the entanglement is weakly in two channels.

5 Conclusion

In this paper, we have examined the interaction between a two-level atom and a boson in a coherent state, subject to a classical magnetic field, Kerr medium and laser pulses. By computing the wavefunction of a quantum model, we have prepared the input state ρ_{in}, which is then transmitted through noisy quantum channels. Two examples of noisy quantum channels, namely the quantum phase flip channel and the double quantum phase flip channel, have been selected for investigation. We have explored the quantum noise and entanglement in these channels by analyzing the output states $\Lambda_{\text{PF}}(\rho_{\text{in}})$ and $\Omega_{\text{DPF}}(\rho_{\text{in}})$, as well as the input state ρ_{in}, using measures such as distance and negativity.

The results indicate that the quantum noise in both channels is relatively low, as the distance between the input and output states is very close. However, the double quantum phase flip channel exhibits the highest level of quantum noise compared to the quantum phase flip channel. Additionally, the negativity, which is an indicator of entanglement, weakens in both channels, signifying a reduction in the degree of entanglement. Finally, our findings demonstrate the impact of noisy quantum channels on quantum noise and entanglement. The investigation sheds light on the behavior of the system under the influence of various factors and provides valuable insights for understanding and characterizing the dynamics of quantum systems in the presence of noise and in future work new types of quantum channels can be discussed.

Funding Open access funding provided by The Science, Technology & Innovation Funding Authority (STDF) in cooperation with The Egyptian Knowledge Bank (EKB).

References

1. Zidan, M.; Aldulaimi, S.; Eleuch, H.: Analysis of the quantum algorithm based on entanglement measure for classifying Boolean multivariate function into novel hidden classes: revisited. Appl. Math. Inf. Sci. **15**, 643–647 (2021). https://doi.org/10.18576/amis/150513
2. Noor, K.I.; Noor, M.A.; Mohamed, H.M.: Quantum approach to starlike functions. Appl. Math. Inf. Sci. **15**(4), 437–441 (2021)
3. Said, T.; Chouikh, A.; Bennai, M.: N two-transmon-qubit quantum logic gates realized in a circuit QED system. Appl. Math. Inf. Sci. **13**, 839–846 (2019)
4. Said, T.; Chouikh, A.; Bennai, M.: Two-step scheme for implementing n two-qubit quantum logic gates via cavity QED. Appl. Math. Inf. Sci. **12**(4), 699–704 (2018)
5. Oleiwi, M.O.; Akoosh, D.J.; Ajeel, S.K.: Evaluation of temperature effects for quantum cascade laser dynamics (QCLS). Int. J. Thin Film Sci. Technol. **12**(2), 141–146 (2023). https://doi.org/10.18576/ijtfst/120209
6. Bogolyubov, N.N., Jr.; Soldatov, A.V.: Time-convolutionless master equation for multi-level open quantum systems with initial system-environment correlations. Appl. Math. **14**(5), 771–780 (2020)
7. Narottama, B.; Shin, S.Y.: Federated quantum neural network with quantum teleportation for resource optimization in future wireless communication. IEEE Trans. Veh. Technol. **72**(11), 14717–14733 (2023). https://doi.org/10.1109/TVT.2023.3280459
8. Bennett, C.H.; Brassard, G.; Crépeau, C.; Jozsa, R.; Peres, A.; Wootters, W.K.: Teleporting an unknown quantum state via dual classical and Einstein-Podolsky-Rosen channels. Phys. Rev. Lett. **70**, 1895–1899 (1993). https://doi.org/10.1103/PhysRevLett.70.1895
9. Bouwmeester, D.; Pan, J.-W.; Mattle, K.; Eibl, M.; Weinfurter, H.; Zeilinger, A.: Experimental quantum teleportation. Nature **390**(6660), 575–579 (1997). https://doi.org/10.1038/37539
10. Pirandola, S.; Eisert, J.; Weedbrook, C.; Furusawa, A.; Braunstein, S.L.: Advances in quantum teleportation. Nat. Photonics **9**(10), 641–652 (2015). https://doi.org/10.1038/nphoton.2015.154
11. Riebe, M.; Häffner, H.; Roos, C.F.; Hänsel, W.; Benhelm, J.; Lancaster, G.P.T.; Körber, T.W.; Becher, C.; Schmidt-Kaler, F.; James, D.F.V.; Blatt, R.: Deterministic quantum teleportation with atoms. Nature **429**(6993), 734–737 (2004). https://doi.org/10.1038/nature02570
12. Ma, X.-S.; Herbst, T.; Scheidl, T.; Wang, D.; Kropatschek, S.; Naylor, W.; Wittmann, B.; Mech, A.; Kofler, J.; Anisimova, E.; Makarov, V.; Jennewein, T.; Ursin, R.; Zeilinger, A.: Quantum teleportation over 143 kilometres using active feed-forward. Nature **489**(7415), 269–273 (2012). https://doi.org/10.1038/nature11472
13. Schumacher, B.: Sending entanglement through noisy quantum channels. Phys. Rev. A **54**, 2614–2628 (1996). https://doi.org/10.1103/PhysRevA.54.2614
14. Shor, P.W.: Scheme for reducing decoherence in quantum computer memory. Phys. Rev. A **52**, R2493–R2496 (1995). https://doi.org/10.1103/PhysRevA.52.R2493
15. Calderbank, A.R.; Shor, P.W.: Good quantum error-correcting codes exist. Phys. Rev. A **54**, 1098–1105 (1996). https://doi.org/10.1103/PhysRevA.54.1098
16. Steane, A.M.: Error correcting codes in quantum theory. Phys. Rev. Lett. **77**, 793–797 (1996). https://doi.org/10.1103/PhysRevLett.77.793
17. Laflamme, R.; Miquel, C.; Paz, J.P.; Zurek, W.H.: Perfect quantum error correcting code. Phys. Rev. Lett. **77**, 198–201 (1996). https://doi.org/10.1103/PhysRevLett.77.198
18. Medina-Armendariz, M.A.; Quezada, L.F.; Sun, G.-H.; Dong, S.-H.: Exploring entanglement dynamics in an optomechanical cavity with a type-v qutrit and quantized two-mode field. Phys. A **635**, 129514 (2024)
19. Kim, H.; Lee, S.-W.; Jeong, H.: Two different types of optical hybrid qubits for teleportation in a lossy environment. Quantum Inf. Process. **15**(11), 4729–4746 (2016). https://doi.org/10.1007/s11128-016-1408-7
20. Jeong, H.; Bae, S.; Choi, S.: Quantum teleportation between a single-rail single-photon qubit and a coherent-state qubit using hybrid entanglement under decoherence effects. Quantum Inf. Process. **15**(2), 913–927 (2016). https://doi.org/10.1007/s11128-015-1191-x
21. Zhang, G.-F.; Ji, A.-L.; Fan, H.; Liu, W.-M.: Quantum correlation dynamics of two qubits in noisy environments: the factorization law and beyond. Ann. Phys. **327**(9), 2074–2084 (2012). https://doi.org/10.1016/j.aop.2012.05.014
22. Guo, Y.-N.; Zeng, K.; Wang, G.-Y.: Pairwise quantum discord for a symmetric multi-qubit system in different types of noisy channels. Int. J. Theor. Phys. **55**(6), 2894–2903 (2016). https://doi.org/10.1007/s10773-016-2920-3
23. Metwally, N.; Abdelaty, M.; Obada, A.-S.: Quantum teleportation via entangled states generated by the Jaynes-Cummings model. Chaos Solitons Fractals **22**(3), 529–535 (2004). https://doi.org/10.1016/j.chaos.2004.02.045
24. El-Hadidy, E.G.; El Anouz, K.; Metwally, N.: The quantum communication efficiency of the fractional anti-Jaynes-Cummings model. Mod. Phys. Lett. A **38**(26n27), 2350126 (2023). https://doi.org/10.1142/S0217732323501262
25. El Anouz, K.; El Aouadi, I.; El Allati, A.; Mourabit, T.: Dynamics of quantum correlations in quantum teleportation. Int. J. Mod. Phys. B **34**(10), 2050093 (2020). https://doi.org/10.1142/S0217979220500939
26. Zidan, N.: Quantum teleportation via two-qubit heisenberg xyz chain. Can. J. Phys. **92**(5), 406–410 (2014). https://doi.org/10.1139/cjp-2013-0404
27. Yu, P.-F.; Cai, J.-G.; Liu, J.-M.; Shen, G.-T.: Teleportation via a two-qubit Heisenberg xyz model in the presence of phase decoherence. Phys. A Stat. Mech. Appl. **387**(18), 4723–4728 (2008). https://doi.org/10.1016/j.physa.2008.03.036
28. Redwan, A.; Abdel-Aty, A.-H.; Zidan, N.; El-Shahat, T.: Dynamics of the entanglement and teleportation of thermal state of a spin chain with multiple interactions. Chaos Interdiscip. J. Nonlinear Sci. **29**(1), 013138 (2019). https://doi.org/10.1063/1.5085784
29. Jaynes, E.; Cummings, F.: Comparison of quantum and semiclassical radiation theories with application to the beam maser. Proc. IEEE **51**(1), 89–109 (1963). https://doi.org/10.1109/PROC.1963.1664
30. Barakat, E.; El-Kalla, I.L.; Abdel-Aty, M.: New prospective on information entropy using different initial states of the atom-field

interaction. Int. J. Mod. Phys. B (2023). https://doi.org/10.1142/S0217979223502788
31. Sivakumar, S.: Nonlinear Jaynes-Cummings model of atom-field interaction. Int. J. Theor. Phys. **43**(12), 2405–2421 (2004). https://doi.org/10.1007/s10773-004-7707-2
32. Seddik, S.; El Anouz, K.; El Allati, A.: Engineering non-classical correlation and teleportation with robust fidelity using Jaynes-Cummings model. Int. J. Geom. Methods Mod. Phys. **19**(02), 2250025 (2022). https://doi.org/10.1142/S0219887822500256
33. El-Kalla, I.: A new approach for solving a class of nonlinear integro-differential equations. Commun. Nonlinear Sci. Numer. Simul. **17**(12), 4634–4641 (2012). https://doi.org/10.1016/j.cnsns.2012.05.016
34. Qiang, W.-C.; Sun, G.-H.; Dong, Q.; Dong, S.-H.: Genuine multipartite concurrence for entanglement of Dirac fields in noninertial frames. Phys. Rev. A **98**, 022320 (2018). https://doi.org/10.1103/PhysRevA.98.022320
35. Dong, Q.; Torres-Arenas, A.J.; Sun, G.-H.; Qiang, W.-C.; Dong, S.-H.: Entanglement measures of a new type pseudo-pure state in accelerated frames. Front. Phys. **14**(2), 21603 (2019)
36. Dong, Q.; Sanchez, M.M.; Sun, G.-H.; Toutounji, M.; Dong, S.-H.: Tripartite entanglement measures of generalized Ghz state in uniform acceleration. Chin. Phys. Lett. **36**(10), 100301 (2019)
37. Su, X.; Tan, A.; Jia, X.; Zhang, J.; Xie, C.; Peng, K.: Experimental preparation of quadripartite cluster and Greenberger-Horne-Zeilinger entangled states for continuous variables. Phys. Rev. Lett. **98**, 070502 (2007). https://doi.org/10.1103/PhysRevLett.98.070502
38. Neves, L.; Lima, G.; Aguirre Gómez, J.G.; Monken, C.H.; Saavedra, C.; Pádua, S.: Generation of entangled states of qudits using twin photons. Phys. Rev. Lett. **94**, 100501 (2005). https://doi.org/10.1103/PhysRevLett.94.100501
39. Gómez, S.; Mattar, A.; Machuca, I.; Gómez, E.S.; Cavalcanti, D.; Farías, O.J.; Acín, A.; Lima, G.: Experimental investigation of partially entangled states for device-independent randomness generation and self-testing protocols. Phys. Rev. A **99**, 032108 (2019). https://doi.org/10.1103/PhysRevA.99.032108
40. Santos, A.C.; Cidrim, A.; Villas-Boas, C.J.; Kaiser, R.; Bachelard, R.: Generating long-lived entangled states with free-space collective spontaneous emission. Phys. Rev. A **105**, 053715 (2022). https://doi.org/10.1103/PhysRevA.105.053715
41. Julsgaard, B.; Kozhekin, A.; Polzik, E.S.: Experimental long-lived entanglement of two macroscopic objects. Nature **413**(6854), 400–403 (2001). https://doi.org/10.1038/35096524
42. Abdel-Aty, M.: Quantum information entropy and multi-qubit entanglement. Progr. Quantum Electron. **31**(1), 1–49 (2007). https://doi.org/10.1016/j.pquantelec.2007.03.002
43. Metwally, N.; El-Amin, A.: Maximum entangled states and quantum teleportation via single cooper pair box. Phys. E Low-dimens. Syst. Nanostruct. **41**(4), 718–722 (2009). https://doi.org/10.1016/j.physe.2008.11.012
44. Ferrie, C.; Morris, R.; Emerson, J.: Necessity of negativity in quantum theory. Phys. Rev. A **82**, 044103 (2010). https://doi.org/10.1103/PhysRevA.82.044103
45. Cornfeld, E.; Sela, E.; Goldstein, M.: Measuring fermionic entanglement: entropy, negativity, and spin structure. Phys. Rev. A **99**, 062309 (2019). https://doi.org/10.1103/PhysRevA.99.062309
46. Leoński, W.; Dyrting, S.; Tanaś, R.: One-photon state generation in a kicked cavity with nonlinear Kerr medium. In: Eberly, J.H., Mandel, L., Wolf, E. (eds.) Coherence and Quantum Optics VII, pp. 425–426. Springer, US, Boston, MA (1996)
47. Leoński, W.; Tanaś, R.: Possibility of producing the one-photon state in a kicked cavity with a nonlinear Kerr medium. Phys. Rev. A **49**, R20–R23 (1994). https://doi.org/10.1103/PhysRevA.49.R20
48. Meystre, P.; Sargent, M.: Elements of Quantum Optics, Springer-Link: Springer e-Books, Springer Berlin Heidelberg, 2007. https://books.google.com.eg/books?id=81GSjqCIIFAC
49. de Azevedo Biagioni, H.: A Nonlinear Theory of Generalized Functions, Lecture Notes in Mathematics, Springer Berlin Heidelberg (2006). https://books.google.com.eg/books?id=cSF6CwAAQBAJ
50. Nielsen, M.A.; Chuang, I.L.: Quantum Computation and Quantum Information, vol. 2. Cambridge University Press, Cambridge (2001)
51. Gyongyosi, L.; Imre, S.: Properties of the quantum channel (2012). arXiv:1208.1270